1/23

ANALYSES OF DRIFT INSTABILITY AND ROCKFALL DUE TO EARTHQUAKE GROUND MOTION AT YUCCA MOUNTAIN, NEVADA: PROGRESS REPORT

Prepared for

Nuclear Regulatory Commission
Contract NRC-02-97-009

Prepared by

Rui Chen

Center for Nuclear Waste Regulatory Analyses
San Antonio, Texas

September 1998

ABSTRACT

Located in the tectonically active Central Basin and Range Province of the North American Cordillera, Yucca Mountain (YM) and the surrounding area will continue to experience earthquake activity. Continuing earthquake activity may affect the integrity and radiological safety of the proposed geological repository for high-level wastes because of possible disruptions to underground openings. A technical issue of concern in the repository performance assessment at YM is potential damage to the waste packages (WPs) emplaced in the drifts by direct rockfall due to earthquake ground motion, particularly because the rock mass surrounding the proposed repository is highly fractured. This report documents the status of an on-going project that studies rockfall due to earthquake ground motion, including assessing the size of rock blocks that can fall, the possibility of multiple rock blocks falling onto a WP simultaneously, and the extent of the potential rockfall region.

Size of individual rock blocks that can fall is controlled by geometrical characteristics of the fracture network, including fracture spacing, orientation, persistence, and trace length. Fracture data collected by the U.S. Department of Energy through various site characterization activities, including those from the full peripheral geological mapping and detailed line survey in the exploratory studies facility drifts, were used to generate irregular fracture patterns representative of the *in situ* fracture patterns at the proposed repository for rockfall analyses. Rockfall phenomena were then analyzed on a drift scale model consisting of a single emplacement drift using the distinct element computer code UDEC Version 3.0. The UDEC Version 3.0 analyses simulated the behavior of an unsupported emplacement drift undergoing repeated earthquake ground motion after subjecting it to *in situ* stress and, for some cases, decayed thermal load generated by the emplaced wastes. In the cases with thermal loading, thermal analyses were conducted for the first 100 yr assuming that thermal stress after 100 yr will not have significant effect on rockfall due to thermal decay. These analyses apply to the postclosure period (i.e., after 100 yr) since rockfall is not considered to affect the WPs during the preclosure period (assuming 100 yr). This is because ground support systems (e.g., concrete liners) will be in place during the preclosure period to protect WPs from rockfall. Modeling results show that, in most cases, more than one rock block fell simultaneously under earthquake ground motion. Fracture pattern and block size have a controlling effect on the number of rock blocks falling simultaneously under a specific episode of ground shaking. In the worst scenario, the whole drift was filled up by falling rock blocks. Future analyses will attempt to estimate the vertical extent of the potential rockfall region using indices such as the amount of explicitly simulated rockfall, fracture shear and normal displacements, and yield of intact rock blocks. Subsequently, a rockfall criterion will be desirable to generally define the vertical extent of the potential region of rockfall without explicit models of rockfall to reduce the number of computer simulations to model rockfall explicitly under various conditions. Such rockfall criterion may be established as a function of fracture pattern, size of *in situ* rock blocks, and level of earthquake ground motion for a specific combination of rock mass thermal-mechanical (TM) properties. Future analyses will also explore the dependence of the rockfall criterion on TM properties and the lateral extent of the potential rockfall area at the repository. These results serve as direct input into performance assessment for evaluating two possible consequences of rockfall: direct rupture of WPs by the impact force of the falling rock blocks and damage to the container outer pack that may accelerate corrosion and reduce the service life of WPs.

3/23

CONTENTS

Section			Page
FIGURES			vii
TABLES			ix
ACKNOWLEDGMENT			xi
1	INTRODUCTION		1-1
2	MODEL DESCRIPTION		2-1
	2.1	INPUT PARAMETERS	2-1
		2.1.1 Fracture Characteristics	2-1
		2.1.2 Thermal Load	2-3
		2.1.3 Thermal-Mechanical Properties	2-6
		2.1.4 Ground Motion	2-7
	2.2	MODEL GEOMETRY AND BOUNDARY CONDITIONS	2-8
	2.3	MODELING APPROACH	2-9
3	MODELING RESULTS		3-1
	3.1	EXPLICIT ROCKFALL	3-1
	3.2	FRACTURE DISPLACEMENT	3-9
	3.3	YIELD OF INTACT ROCK BLOCKS	3-9
4	DISCUSSIONS AND FUTURE WORK		4-1
	4.1	EFFECT OF FRACTURE PATTERN ON ROCKFALL	4-1
	4.2	EFFECT OF SEISMIC TIME HISTORY ON ROCKFALL	4-2
	4.3	EFFECT OF INTACT ROCK AND FRACTURE THERMAL-MECHANICAL PROPERTIES	4-2
	4.4	EFFECT OF MODEL SETUP ON ROCKFALL	4-2
	4.5	EXPLICIT MODELING OF ROCKFALL AND ROCKFALL CRITERIA	4-2
5	REFERENCES		5-1

4/23

FIGURES

Figure		Page
1-1	Integrated seismic hazard results: summary hazard curves for horizontal peak ground acceleration (Wong and Stepp, 1998)	1-2
2-1	Determination of primary fracture sets (TSw2 Exploratory Studies Facility Main Drift) (Pye et al., 1997)	2-2
2-2	Time decay heat flux from a 44-Boiling Water Reactor and a high-level waste package and UDEC Version 3.0 input based on a best exponential fit using a single decay constant	2-6
2-3	UDEC Version 3.0 model showing block geometry and a particular fracture pattern (case C)	2-9
3-1	Explicit rockfall generated by dynamic simulation after subjecting to one episode of earthquake ground motion for case A (unheated drift)	3-2
3-2	Explicit rockfall generated by dynamic simulation after subjecting to one episode of earthquake ground motion for case B (unheated drift)	3-3
3-3	Explicit rockfall generated by dynamic simulation after subjecting to one episode of earthquake ground motion for case C (unheated drift)	3-4
3-4a	Explicit rockfall generated by thermal and dynamic simulation for case B1 (heated drift) after 100 yr of thermal loading	3-5
3-4b	Explicit rockfall generated by thermal and dynamic simulation for case B1 (heated drift) after 100 yr of thermal loading and one episode of earthquake ground motion	3-6
3-5a	Explicit rockfall generated by thermal and dynamic simulation for case C1 (heated drift) after 100 yr of thermal loading	3-7
3-5b	Explicit rockfall generated by thermal and dynamic simulation for case C1 (heated drift) after 100 yr of thermal loading and one episode of earthquake ground motion	3-8
3-6a	Distribution of fracture shear displacement after drift excavation for case A. Each solid line represents 0.25 mm shear displacement	3-10
3-6b	Distribution of fracture shear displacement after one episode of earthquake ground motion for case A. Each line represents 0.25 mm shear displacement	3-11
3-7a	Distribution of opened fractures for case C (in red) after draft excavation	3-12
3-7b	Distribution of opened fractures for case C (in red) after one episode of earthquake ground motion	3-13

5/23

TABLES

Table		Page
2-1	UDEC Version 3.0 parameters used to generate fracture patterns	2-3
2-2	Six possible spent nuclear fuel waste package combinations and associated drift and waste package spacings (U.S. Department of Energy, 1998)	2-4
2-3	Average heat flux at 42.5 MTU/acre thermal load for a unit cell (the sum of a 44-Boiling Water Reactor and a high-level waste package)	2-5
2-4	Intact rock and fracture thermal-mechanical properties (Ahola et al., 1996)	2-7

ACKNOWLEDGMENT

The work described in this report was performed by the Center for Nuclear Waste Regulatory Analyses (CNWRA) for the Nuclear Regulatory Commission (NRC) under contract number NRC-02-97-009, on behalf of the NRC Office of Nuclear Material Safety and Safeguards, Division of Waste Management. The report is an independent product of the CNWRA and does not necessarily reflect the views or regulatory position of the NRC.

The author would like to thank Drs. S. Hsiung and B. Sagar for their technical and programmatic reviews. The author is also thankful to L. Selvey for skillful typing of the report and to B. Long who provided a full range of expert editorial services in the preparation of the final document.

QUALITY OF DATA, ANALYSES, AND CODE DEVELOPMENT

DATA: All CNWRA-generated data contained in this report meet quality assurance (QA) requirements described in the CNWRA QA Manual. Sources for other data should be consulted for determining the level of quality for those data. Several utility software packages developed at the CNWRA were used for analyses of data contained in this report. These software packages fall under the categories covered by QAP-014, Documentation and Verification of Routine Calculations, and are not controlled by configuration management procedure TOP-018, Development and Control of Scientific and Engineering Software.

ANALYSES AND CODES: The distinct element code UDEC Version 3.0, used for all of the thermal-mechanical and dynamic analyses, is controlled under the CNWRA software QA procedure TOP-018.

7/23

1 INTRODUCTION

The proposed geological repository for high-level waste (HLW) at Yucca Mountain (YM), Nevada, is located in the tectonically active central Basin and Range Province of the North American Cordillera (Wernicke, 1992). Presence of numerous Quaternary faults, volcanoes, and historic seismicity is indicative of the state of activity of the region. The recent, most sophisticated probabilistic seismic hazard analyses to date at YM conducted by the U.S. Department of Energy (DOE) through expert elicitation show that the mean horizontal peak ground acceleration is about 0.55 g for a 10,000-yr return period earthquake and 1.32 g for a 100,000-yr return period earthquake [figure 1-1 from Wong and Stepp (1998)]. Such potential earthquake activities may affect the integrity and radiological safety of the proposed repository because of possible disruptions to underground openings, particularly because the rock mass surrounding the proposed repository is highly fractured and contains irregular fracture patterns (Brechtel et al., 1995; Lin et al., 1993; Spengler et al., 1984, 1981, 1980, 1979; Scott and Castellanos, 1984; Sweetkind and Williams-Stroud, 1996; Beason, 1997; Anna, 1998; Pye et al., 1997). A technical issue of concern in the repository performance assessment at YM is potential damage to the waste packages (WPs) emplaced in the drifts by direct rockfall due to earthquake ground motion. The objective of this report is to study such rockfall, including assessing the size of rock blocks that can fall, the possibility of multiple rock blocks falling onto a WP simultaneously, and the extent of the potential rockfall region.

Size of individual rock blocks that can fall is controlled by geometrical characteristics of the fracture network, including fracture spacing, orientation, persistence, and trace length. Fracture data collected by the DOE through various site characterization activities, including those from the full peripheral geological mapping and detailed line survey in the exploratory studies facility drifts, were analyzed. The DOE considerations (Pye et al., 1997) of primary fracture sets based on stereo graphic projections (Schmidt equal area lower hemisphere projection) were used to generate irregular fracture patterns representative of the *in situ* fracture patterns at the proposed repository for rockfall analyses. Rockfall phenomena were then analyzed on a drift scale model consisting of a single emplacement drift using the distinct element computer code UDEC Version 3.0 (Itasca Consulting Group, Inc., 1996). The UDEC Version 3.0 analyses simulated the behavior of an unsupported emplacement drift undergoing repeated earthquake ground motion after subjecting it to *in situ* stress and, for some cases, decayed thermal load generated by the emplaced wastes. In the cases with thermal loading, thermal analyses were conducted for only the first 100 yr assuming that thermal stress after 100 yr will not have a significant effect on rockfall due to thermal decay. These analyses apply to the postclosure period (after 100 yr) since rockfall is not considered to affect the WPs during the preclosure period (assuming 100 yr). This is because ground support systems (e.g., concrete liners) will be in place during the preclosure period to protect WPs from rockfall.

Chapter 2 of this report gives a detailed model description, including input parameters and rationales for selecting them, model geometry and boundary conditions, and modeling approach. Chapter 3 presents modeling results of explicit rockfall, fracture displacement and opening, and yield of intact rock blocks. Chapter 4 discusses sensitivity of simulated rockfall to factors such as fracture pattern, seismic time history, intact rock and fracture TM properties, and model setup. A general discussion of explicit modeling of rockfall and the possibility of establishing a rockfall criterion is also given in chapter 4. This is a preliminary study on modeling explicit rockfall. Chapter 4 also discusses challenges and efforts for further studies. Results of these studies will serve as direct inputs into performance assessment for evaluating two possible consequences of rockfall: direct rupture of WPs by the impact force of the falling rock blocks and damage to the container outer pack that may accelerate corrosion and reduce the service life of WPs.

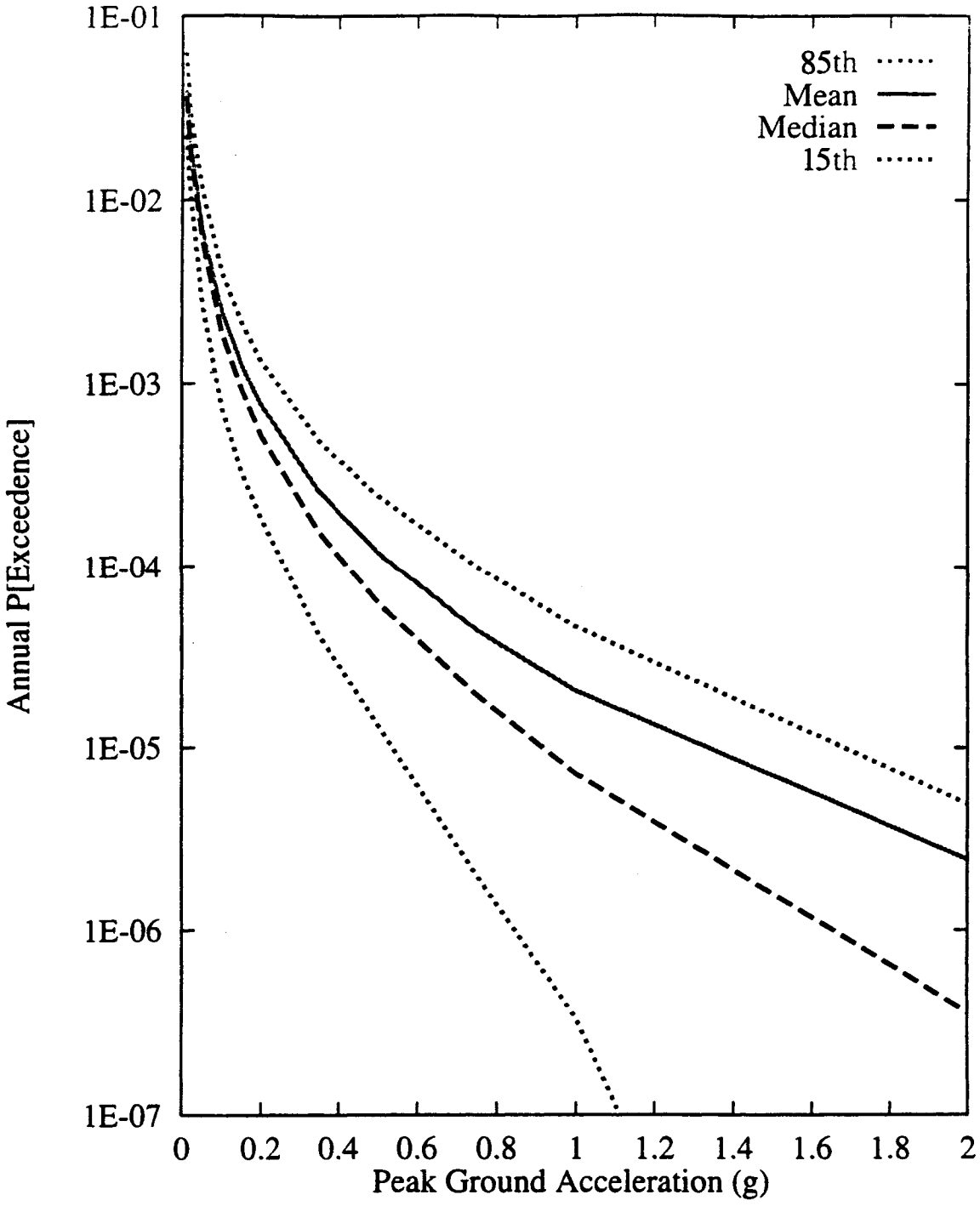

Figure 1-1. Integrated seismic hazard results: summary hazard curves for horizontal peak ground acceleration (Wong and Stepp, 1998)

2 MODEL DESCRIPTION

2.1 INPUT PARAMETERS

Important input to the dynamic analyses include fracture patterns, ground motion time histories, thermal loading from emplacement wastes, and rock mass and fracture TM properties. These input parameters are selected based mainly on the DOE site characterization data and repository design considerations as detailed in the following paragraphs.

2.1.1 Fracture Characteristics

Abundant information has been obtained on fracture characteristics at YM by the DOE through site characterization activities. Fracture data have been collected through core hole exploration (Brechtel et al., 1995; Lin et al., 1993; Spengler et el., 1984, 1981, 1980, and 1979; Scott and Castellanos, 1984), surface mapping (Sweetkind and Williams-Stroud, 1996), and full-periphery geological mapping and detailed line survey in the Exploratory Studies Facilities (ESF) (Beason, 1997; Anna, 1998). Detailed analyses of these fracture data are still in progress at the CNWRA, including analyses of *in situ* block size distributions and statistical summaries of fracture orientation, spacing, and persistence. For the current study, the DOE analyses (Pye et al., 1997) of fracture orientations, frequencies, and fracture sets for the TSw2 based on the detailed line survey data along the ESF main drift were used as the basis to generate fracture patterns for dynamic analyses.

Using stereo graphic projections (Schmidt equal area lower hemisphere projection), the DOE determined three primary fracture sets (figure 2-1 from Pye et al., 1997). It was also observed that fracture spacings follow log-normal distributions. For the current study, UDEC Version 3.0 command JSET was used to generate an approximation of these three fracture sets. It should be noted that there are a number of limitations in the UDEC Version 3.0 fracture generator including (i) it is limited to two dimensions (2D), (ii) fracture spacing, orientation, trace length, and persistence are assumed to have uniform distributions, and (iii) UDEC Version 3.0 is not capable of handling fractures that do not completely intersect a block. Ideally, a three-dimensional (3D) fracture generator that can account for a variety of distribution types should be used to generate fractures in 3D and obtain the required 2D cross section from the 3D model for mechanical analyses. Alternatively, fracture patterns on a typical cross section from the underground mapping data may be used to digitize the fractures and manually input them into the UDEC Version 3.0 model using UDEC Version 3.0 command CRACK. These options will be further explored in the future when more fracture analysis data become available.

Three fracture patterns were generated for thermal-dynamic analyses. All three cases were generated using as much DOE stereo graphic analysis results as possible under the limitations of UDEC Version 3.0 as described previously; that is, estimating a mean and a deviation value for fracture spacing and orientation based on information provided in figure 2-1 for each of the three primary fracture sets and using the estimated mean and deviation to generate a fracture pattern in UDEC Version 3.0. It is to be noted that individual judgment played an important role in selecting the mean and deviation for the three fracture sets showing in figure 2-1. The purpose of selecting three cases for analyses was to obtain a snap shot of the effect of fracture pattern on rockfall, not to systematically cover all the possible fracture patterns at the repository. Also, fracture trace length and persistence are mainly assumed data. These cases are referred to as cases A through C. Only two fracture sets were assumed for case A, whereas cases B and C had three fracture sets. Table 2-1 presents the UDEC Version 3.0 parameters used to generate these fracture patterns.

DETERMINATION OF PRIMARY JOINT SETS
TSw2 MAIN DRIFT

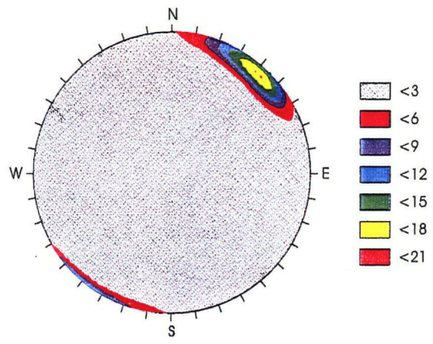

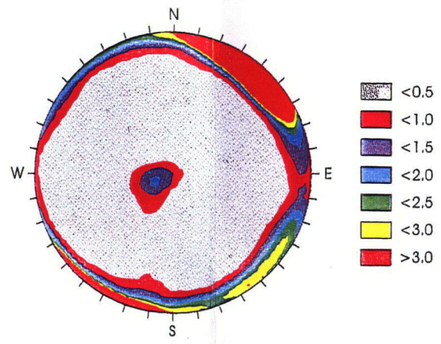

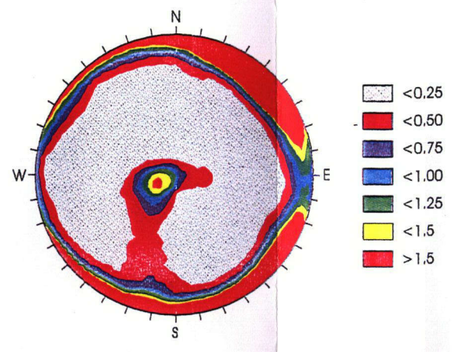

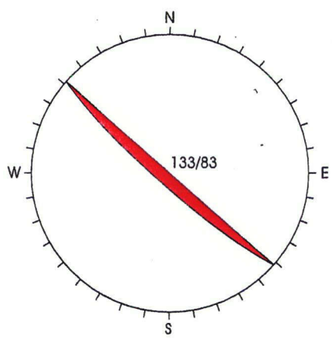

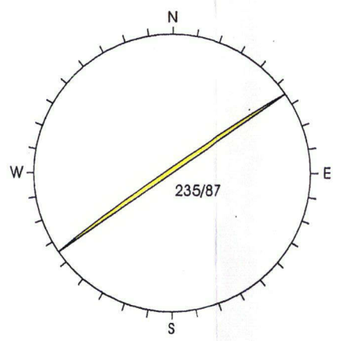

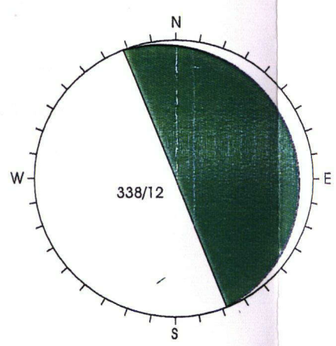

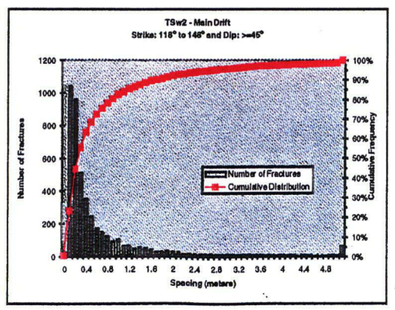

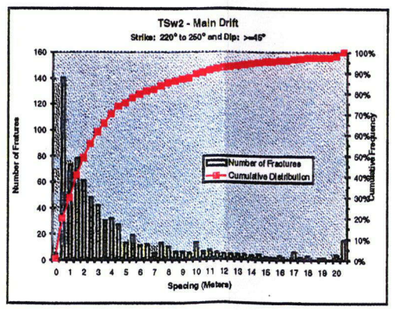

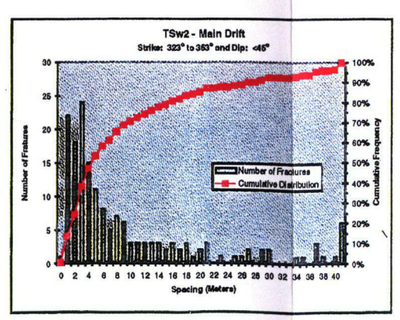

Figure 2-1. Determination of primary fracture sets (TSw2 Exploratory Studies Facility Main Drift) (Pye et al., 1997)

Table 2-1. UDEC Version 3.0 parameters used to generate fracture patterns

Case	Fracture Set	Angle From X Axis (degree)		Trace Length (m)		Gap Length (m)		Joint Spacing (m)	
		Mean	Deviation	Mean	Deviation	Mean	Deviation	Mean	Deviation
A	1st	85	10	7.5	1	0	0	0.4	0.1
	2nd	20	5	5	1	0	0	0.75	0.1
B	1st	85	10	12	4	0	0.1	0.3	0.05
	2nd	20	8	6	2	0	0.1	0.75	0.4
	3rd	110	10	12	4	0	0.1	1.8	0.5
C	1st	85	10	7.5	1	0	0	0.4	0.1
	2nd	20	5	5	1	0	0	0.75	0.1
	3rd	110	10	12	4	0	0.1	1.8	0.5

2.1.2 Thermal Load

The DOE current thermal loading strategy uses the concept of areal mass load (AML). AML refers to the mass of waste emplaced within a unit area occupied by WPs in the repository. Units are in metric tons of uranium per acre (MTU/acre). The Controlled Design Assumptions Document (Civilian Radioactive Waste Management System, Management and Operating Contractor, 1995) describes the assumptions for the thermal loading strategy for YM using the AML as a unit of measure. It states that surface, subsurface and WP designs will be based on a reference mass loading range of 80–100 MTU/acre, with 85 MTU/acre the highest AML that will result in rock temperatures below the geochemical thermal limit or the thermal goals [i.e., the temperature at the average top of the zeolite layer (170 m beneath the potential emplacement area) shall not exceed 90 °C (Civilian Radioactive Waste Management System, Management and Operating Contractor, 1996a)] (U.S. Department of Energy, 1998). Therefore, for the current modeling study, 85 MTU/acre AML was used. To maintain this mass density and consider the prescribed dimensions of the WPs to be disposed at YM, the DOE proposed six possible arrangements of WPs and calculated associated drift and WP spacings as shown in table 2-2, where there is an HLW package between every adjacent spent nuclear fuel (SNF) WPs [containing 21-Pressurized Water Reactor (PWR), 44-Boiling Water Reactor (BWR), or 12-PWR WPs]. The DOE analysis shows that to ensure every space between all SNF WPs can be arranged to accommodate an HLW package while the 85 MTU/acre is still maintained, a uniform drift spacing of 28 m needs to be planned for the entire repository. For 28 m drift spacing, the WP spacing is calculated to be 13.26 m. The heat mass content [$Q(t)$] is the sum of a 44-BWR package [$Q(t)_{44\,BWR}$] and a HLW package [$Q(t)_{HLW}$] (table 2-2) for a single drift and a one-unit cell width (U.S. Department of Energy, 1998):

$$Q(t) = Q(t)_{44BWR} + Q(t)_{HLW} \qquad (2\text{-}1)$$

Table 2-2. Six possible spent nuclear fuel waste package combinations and associated drift and waste package spacings (U.S. Department of Energy, 1998)

Sequence Number	Waste Package Arrangement	Maximum Drift Spacing (m)	Waste Package Spacing (m)
1	21-PWR HLW 44-BWR	30	13.28
2	21-PWR HLW 21-PWR	32	13.3
3	21-PWR HLW 12-PWR	25	13.67
4	44-BWR HLW 44-BWR	28	13.26
5	44-BWR HLW 12-PWR	23	13.68
6	12-PWR HLW 12-PWR	19	13.58
Note: PWR = Pressurized Water Reactor, HLW = High-Level Waste, and BWR = Boiling Water Reactor			

The average thermal decay for a 44-BWR package and a n HLW package given in table V-1 of DOE (1998) was used in calculating $Q(t)$. These values are represented in table 2-3. Assuming that heat is uniformly distributed on the drift wall, the decay heat flux $q(t)$ is calculated as

$$q(t) = \frac{Q(t)}{\pi D L_{wp}} \tag{2-2}$$

where D is drift diameter (5 m) and L_{wp} is WP spacing (13.26 m). Version 3.0 of UDEC currently allows a thermal flux boundary condition to be input as a constant or simple exponentially decaying flux with a single decay coefficient of the form

$$q(t) = q_0 \exp(-\alpha t) \tag{2-3}$$

where q_0 is the initial surface heat flux (W/m^2) applied to the drift wall at time of emplacement and α is the decay constant (1/s). The initial heat flux was calculated to be 21.59 W/m^2 for 42.5 MTU/acre (or 43.18 W/m^2 for 85 MTU/acre) thermal load according to Eq. (2-2) and the decay constant was determined to be 3.2197×10^{-10}/s by a best-fitted curve (figure 2-2).

It is to be noted that this modeling approach is an approximation. First, in reality, heat transfer from the WP to surrounding rock in an unbackfilled drift would consist of a combination of radiative heat transfer to the wall of the emplacement drift as well as conductive heat transfer to the tunnel floor through the WP support system. Depending on if the unbackfilled drifts are ventilated, heat transfer could also take place in

Table 2-3. Average heat flux at 42.5 MTU/acre thermal load for a unit cell (the sum of a 44-Boiling Water Reactor and a high-level waste package)

Time (y)	44 BWR (W/pkg)	HLW (W/pkg)	44 BWR+HLW (W/pkg)	Flux(W/m^2)
0	7493.21	1496.00	8989.21	21.59
5	6651.67	2350.00	8001.67	19.22
10	6051.52	1204.00	7255.52	17.43
20	5121.87	998.00	6119.87	14.70
30	4400.25	792.00	5192.25	12.47
40	3834.48	693.60	4528.08	10.88
50	3375.95	595.20	3971.15	9.54
60	3008.99	496.8	3505.79	8.42
70	2712.55	398.4	3110.95	7.47
80	2467.95	300.00	2767.95	6.65
90	2271.75	276.8	2548.55	6.12
100	2103.07	253.60	2356.67	5.66
150	1597.44	137.60	1735.04	4.17
200	1337.74	60.16	1397.9	3.36
300	1062.96	25.6	1088.56	2.61
400	895.55	16.13	911.68	2.19
500	776.30	10.54	786.84	1.89
600	679.93	9.26	689.19	1.66
700	604.73	7.98	612.71	1.47
800	539.66	6.70	546.36	1.31
900	487.87	5.42	493.29	1.18
1000	444.29	4.40	448.69	1.08
2000	230.59	2.88	233.47	0.56
3000	176.92	52.64	179.56	0.43
4000	157.32	2.40	1559.72	0.38
5000	146.55	2.16	148.71	0.36
6000	135.66	2.07	137.73	0.33
7000	127.07	1.98	129.05	0.31
8000	119.01	1.89	120.90	0.29
9000	112.33	1.81	114.14	0.27
10000	106.61	1.72	108.33	0.26

Note: PWR = Pressurized Water Reactor, HLW = High-Level Waste, and BWR = Boiling Water Reactor

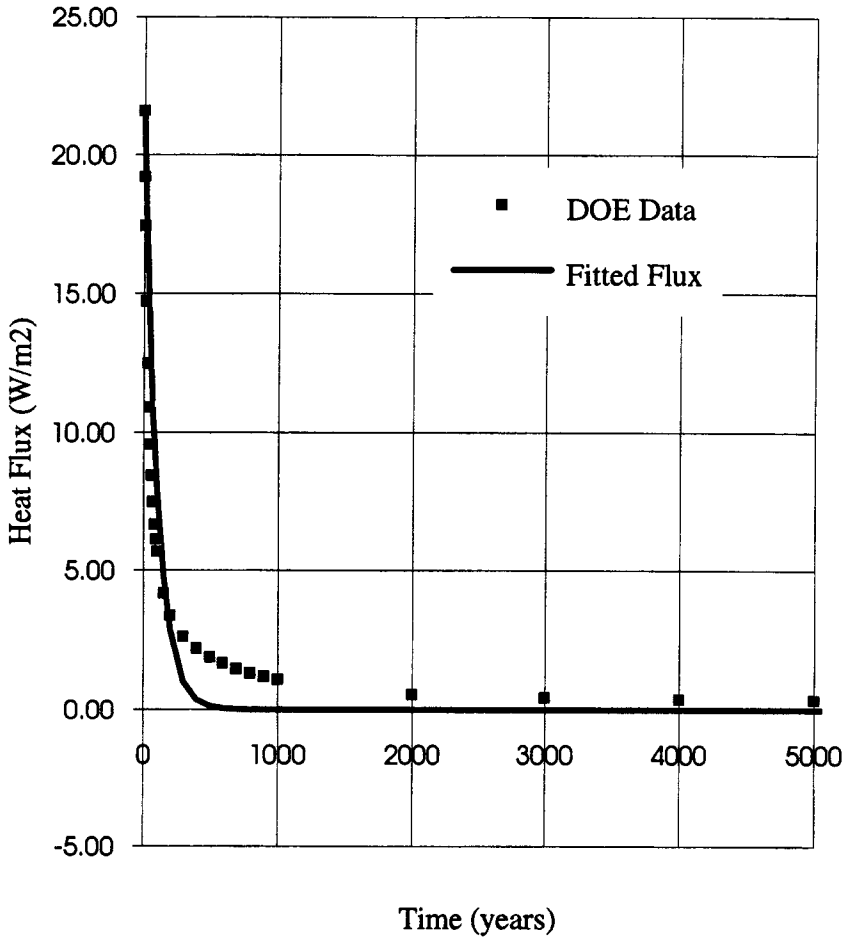

Figure 2-2. Time decay heat flux from a 44-Boiling Water Reactor and a high-level waste package and UDEC Version 3.0 input based on a best exponential fit using a single decay constant. These curves represent necessary two-dimensional tunnel wall heat flux required to establish mass loading of 42.5 MTU/acre.

the form of forced convection. Because Version 3.0 of UDEC is incapable of modeling cavity radiation (i.e., currently it handles only boundary radiation to an infinite domain), it was decided to neglect modeling of the WP itself and apply the volumetric heat generated directly as a heat flux to the drift wall. In essence, the analysis neglects heat removal from ventilation. Second, as stated earlier, a best exponential fit using a single decay constant was used to approximate the heat generation rate (decay). In actuality, a number of exponentially decaying terms are usually required. For instance, a recent DOE TM analysis (TRW Environmental Safety Systems, Inc., 1995) used a decaying source term with four decay coefficients.

2.1.3 Thermal-Mechanical Properties

TM properties for the current study were selected from a specific case of a previous parametric drift stability study (case 12 from Ahola et al., 1996). These parameter values are presented in table 2-4 for intact rock and fractures. This combination of intact and fracture TM properties caused relatively significant yielding and large shear displacement along fractures (Ahola et al., 1996). These parameter values represent an upper bound value for intact rock cohesion and intact rock Young's modulus; a lower bound value for

Table 2-4. Intact rock and fracture thermal-mechanical properties (Ahola et al., 1996)

Parameters	Parameter Values	Unit
Young's Modulus	32	GPa
Poisson's Ratio	0.21	–
Rock Friction Angle	20	Degrees
Rock Cohesion	43	MPa
Rock Tensile Strength	5	MPa
Rock compressive Strength	166	MPa
Rock Density	2297	kg/m^3
Fracture Friction Angle	38	degrees
Fracture Cohesion	0.08	MPa
Fracture Tensile Strength	0.04	MPa
Fracture Normal and Shear Stiffness	1.0×10^{-5}	MPa/m
Fracture Angle of Friction	0.04	–
Thermal Expansion Coefficient	6×10^{-6}	K^{-1}
Thermal Conductivity	2.1	W/m-K
Specific Heat	932	J/Kg-K

fracture friction angle, thermal expansion coefficient, and intact rock friction angle; and an average value for the other parameters. As detailed in Ahola et al. (1996), the upper and lower bound and average values of various parameters were selected based on information available from a number of sources including the DOE YM Reference Information Base (U.S. Department of Energy, 1994), borehole drilling data from the YM region (Brechtel et al., 1995), as well as from the DOE thermal study reports (TRW Environmental Safety System, Inc., 1994a,b, 1995, 1996).

2.1.4 Ground Motion

Since the main purpose of the current study is to establish a strategy to explicitly model rockfall, seismic ground motion input was kept simple. A simple sigmoidal dynamic signal was used, corresponding to a maximum peak ground acceleration of approximately 0.4 g. Potential effects of various characteristics of a more realistic earthquake time history will be investigated in the future. The dynamic signal was applied to the base of the model as a vertically propagating compressive stress wave.

2.2 MODEL GEOMETRY AND BOUNDARY CONDITIONS

Similar to previous studies (Ahola et al., 1996), selections of geometric models and boundary conditions were based on the assumption of multiple parallel emplacement drifts and a rock mass that is highly fractured. The study simulated a single emplacement drift placed in the middle of a group of similar emplacement drifts parallel to each other. The emplacement drifts were assumed to be long enough so the plane-strain condition applies. All the fractures were assumed to be 2D and had strikes parallel to the drift. Drift diameter was 5 m and drift spacing 28 m.

Figure 2-3 depicts the geometric model comprised of discrete element blocks for a particular fracture pattern analyzed (case C). The model extended vertically from ground surface (about 317 m above the repository horizon) to approximately the groundwater level (about 350 m below the repository level). At such extent, heat flux due to emplaced WPs is almost zero and the ambient temperatures applied along the upper and lower boundaries do not influence the results in the area around the drift for the selected simulation time of 100 yr. To maintain a reasonably small number of blocks and finite difference zones and therefore a workable problem size, only a region approximately one drift diameter in the rock mass was modeled as having the specified fracture spacings. Beyond this region, the size of the blocks was gradually scaled up, while maintaining a comparable fracture pattern. Zoning of the individual blocks was also scaled accordingly. Rock support around the emplacement drift was not modeled. Also, the emplacement drifts were assumed not ventilated.

The vertical boundaries represented lines of symmetry based on the assumption of multiple parallel emplacement drifts, and therefore, were assigned zero horizontal displacement and zero heat flux conditions. The top boundary representing the ground surface was stress free allowing for upward thermal expansion. The bottom boundary was fixed in the vertical direction. Temperature at the top boundary was fixed at 18.7 degrees and at the bottom boundary was fixed at 34.2 degrees. Geothermal gradient was ignored because it has a negligible effect on rockfall induced by either thermal or dynamic stresses. The *in situ* vertical stress at the repository horizon was set to be 7.0 MPa based on average measured values in the DOE advanced conceptual design (Civilian Radioactive Waste Management System, Management and Operating Contractor, 1996b). The vertical stress gradient with depth was assumed 0.0221 MPa/m based on a uniform rock density of 2257 kg/m^3. The *in situ* horizontal stress was assumed related to the vertical stress by Poisson's ratio. The Poisson's ratio of 0.21 (see table 2-4) resulted in a horizontal stress gradient of 0.00587 MPa/m along the vertical and a 1.89 MPa horizontal stress at the repository level.

For dynamic analyses, a smaller submodel of the original problem domain was used to reduce the size of the problem and computational time required. This was achieved after the initial TM analyses. Solutions of stresses, temperature, and displacements from the TM analyses were used in the initial conditions for the subsequent dynamic analyses. The submodel extended 50 m above and below the repository horizon (figure 2-3). For this preliminary study, only a vertically propagating compressive wave was applied. Therefore, the vertical boundaries remained rollered, as was the case for the TM analysis. After first solving for the new boundary stresses (from the solution of the TM model) to be applied to these two boundaries of the submodel after deleting the upper and lower portions from the large TM model, viscous nonreflecting boundary conditions were applied to the top and base of the dynamic model. For the base of the model, this required imputing the earthquake signal as a stress wave rather than as a velocity time history since two velocity boundary conditions (i.e., viscous damping and earthquake velocity time history) cannot be applied at the same boundary. As a result, reflections from the drifts were allowed to pass through the base.

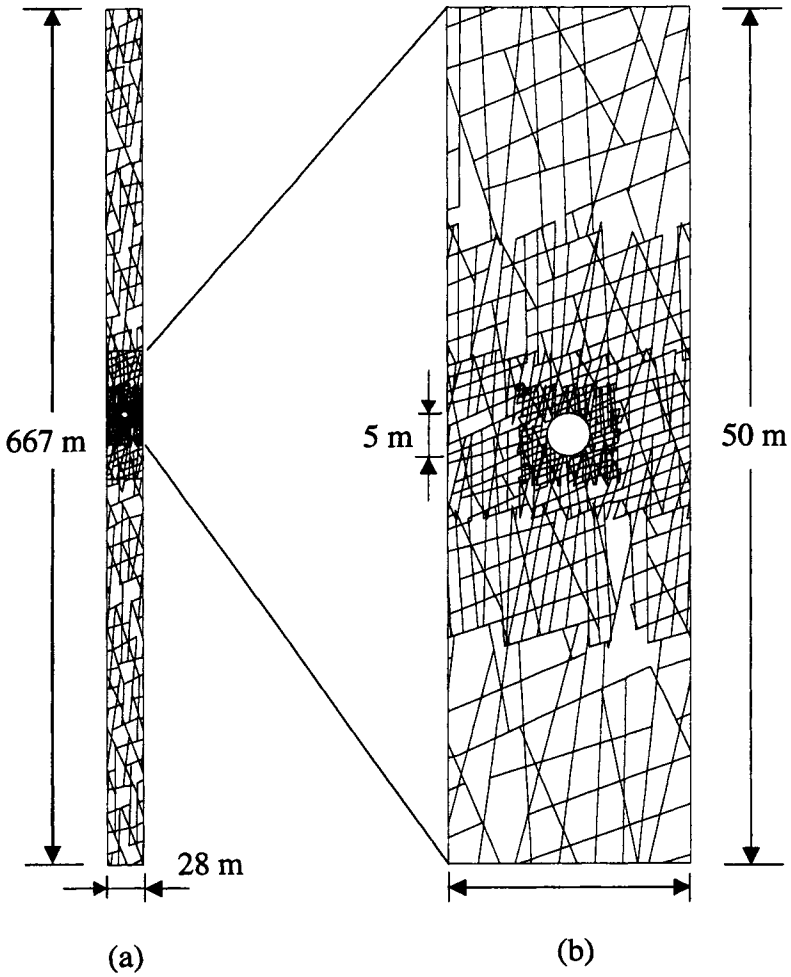

Figure 2-3. UDEC Version 3.0 model showing block geometry and a particular fracture pattern (case C). Fractures were assumed to be parallel in the third dimension and perpendicular to the cross section analyzed. (a) Full model for thermal-mechanical analyses. (b) Submodel for dynamic analyses.

2.3 MODELING APPROACH

The modeling started by obtaining an initial model equilibrium under *in situ* stress. After the model reached the initial equilibrium, the tunnel was excavated and a new model equilibrium reached. After these initial analyses, the mechanical time was reset to zero for the TM analysis. UDEC Version 3.0 uses a sequential coupling approach in conducting a TM analyses. This approach consists of running the thermal analysis for a period of time during which the nodal or grid-point temperature is updated. The thermal time is then held fixed while mechanical cycling is conducted to update zone stresses, nodal displacements, and block rotations to reach a new mechanical equilibrium. In such analyses, thermal time is the actual simulation time while the mechanical time is a pseudo-time for the intermediate calculations. An implicit thermal solution scheme based on the Crank-Nicholson method (Itasca Consulting Group, Inc., 1996) was chosen to allow the user to specify a thermal time-step.

For each fracture pattern listed in table 2-1, two analyses were performed. The first (cases A, B, and C) assumes no thermal load and the models were subjected to only *in situ* stress and dynamic load. For the second set of analyses (cases A1, B1, and C1), the time-decay thermal load described in section 2.1.2 was applied to the emplacement drift for 100 yr. This corresponds to the repository preclosure time period. At 100 yr, dynamic analysis was conducted to model the effect of an earthquake. When desirable, the seismic load was repeated once to look at the effect of repetitive seismic load on rockfall.

3 MODELING RESULTS

Modeling results are discussed using explicit rockfall, fracture shear and normal displacements, yield of intact rock blocks, and the relationship among rockfall, fracture displacement, and yielding. A combination of these observations may provide indications of the maximum extent of the potential rockfall region. The observations may also be used as indices for establishing a rockfall criterion in future studies. Both thermal loading levels of 42.5 MTU/acre and 85 MTU/acre were analyzed, although only the latter case was presented in this chapter since these different thermal loading levels did not appear to affect explicit rockfall significantly. The effect of thermal loading level on stresses and displacements will be discussed in detail in the future.

3.1 EXPLICIT ROCKFALL

Explicit rockfall generated by dynamic simulation after subjecting to one episode of earthquake ground motion is shown for cases A (figure 3-1), B (figure 3-2), and C (figure 3-3). Rockfall in case A was limited to the upper-right corner of the drift. The drift appeared to be in a rather stable state after the first rockfall because a second episode of earthquake ground motion did not induce further rockfall. Case C had the most extensive rockfall. Rock blocks within a wide region extending 3–3.5 m into the roof area fell into the drift simultaneously after one episode of seismic load, causing the entire opening to collapse. Comparison of the cross sectional area of the opening with the area of the simulated rockfall region indicated this particular rockfall event could fill most of the drift with falling blocks and completely bury the WP. The drift appeared to be unstable after the first episode of seismic load and rock blocks continued to fall off. In case B, the upper-right corner and the first layer of blocks fell off after the first episode of seismic load. The extension of the region of rockfall on the upper-right corner was much greater than that of case A. Continuing analysis showed the upper-right corner was rather unstable, causing collapse of the drift wall on the right-hand side.

As indicated by fracture patterns shown in figures 3-1 through 3-3 and fracture parameters shown in table 2-1, among the three cases, the fracture pattern was the simplest in case A, which included two fracture sets. The first two fracture sets in case B were essentially the same as those in case A, except case B included a third fracture set oriented about 110 degrees from the x-axis. Although this third fracture set had large spacings, its inclusion in the model increased the amount of simulated rockfall significantly. The fracture pattern in case C was similar to that in case B, however, block size was smaller and more irregular in the roof region. These comparisons indicate that the more irregular the fracture pattern, the more extensive the rockfall. Rockfall also shows dependence on block size: the smaller the block size, the more extensive the rockfall. Further analyses are necessary to confirm these observations.

In the case of heated drifts (i.e., conducting TM analyses for 100 yr prior to dynamic analyses), some rock blocks fell during thermal loading stage. For example, the blocks on the upper-right corner in case A1 fell off during the thermal loading and then the opening appeared to be stable with no further falling blocks during seismic load. In case B1, blocks on the upper-right corner loosened during thermal loading and eventually fell off at the early stage of seismic loading (figures 3-4a,b). It is interesting to note that the region involving rockfall for the case of heated drift is actually smaller than that in the case of unheated drift. Repetitive seismic load did not cause further rockfall. A similar phenomenon was also observed in case C1. Blocks in the roof region in case C1 loosened during thermal loading and gradually fell off during the early stage of seismic loading (figures 3-5a,b). Similar to case B1, the region involving rockfall in the case of heated drift is somewhat smaller than that of an unheated drift during the first episode of seismic loading. Rockfall continued during the subsequent modeling, however, and the opening appeared to be unstable as was the case in the unheated drift.

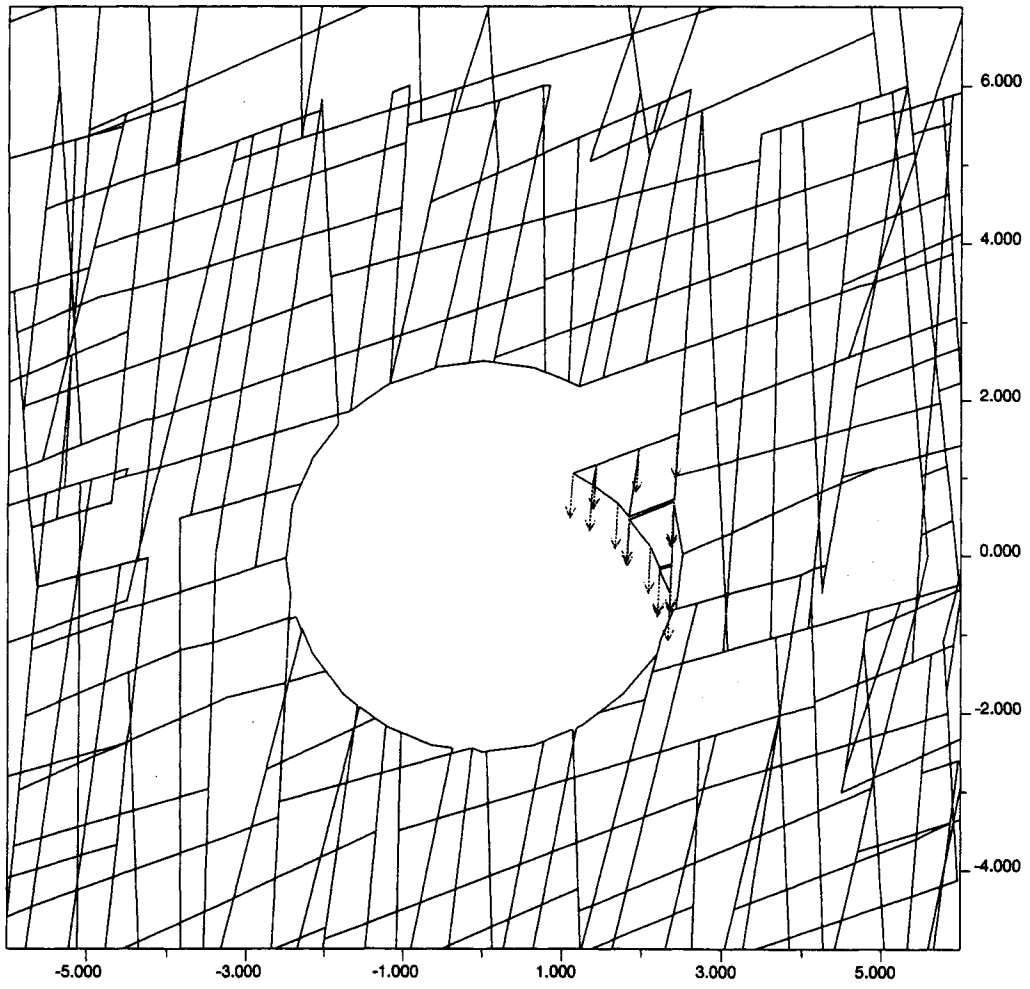

Figure 3-1. Explicit rockfall generated by dynamic simulation after subjecting to one episode of earthquake ground motion for case A (unheated drift)

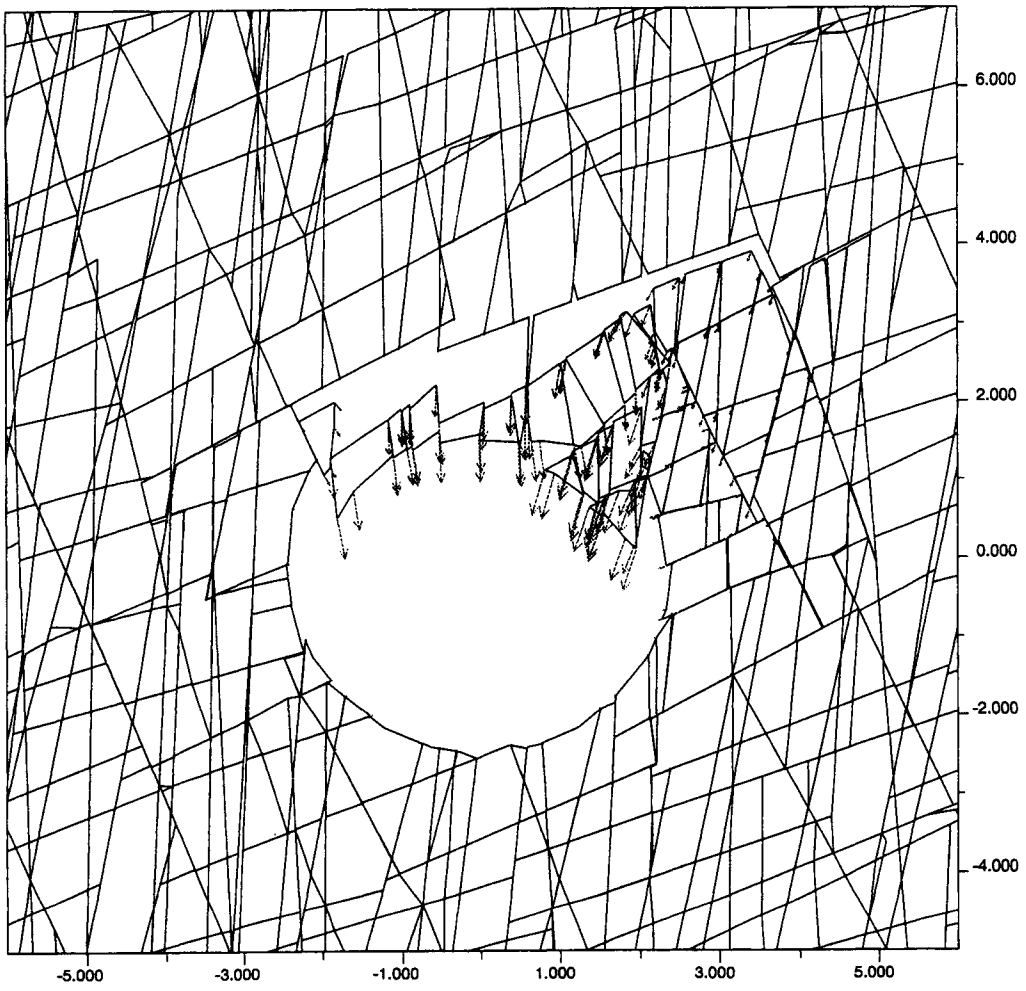

Figure 3-2. Explicit rockfall generated by dynamic simulation after subjecting to one episode of earthquake ground motion for case B (unheated drift)

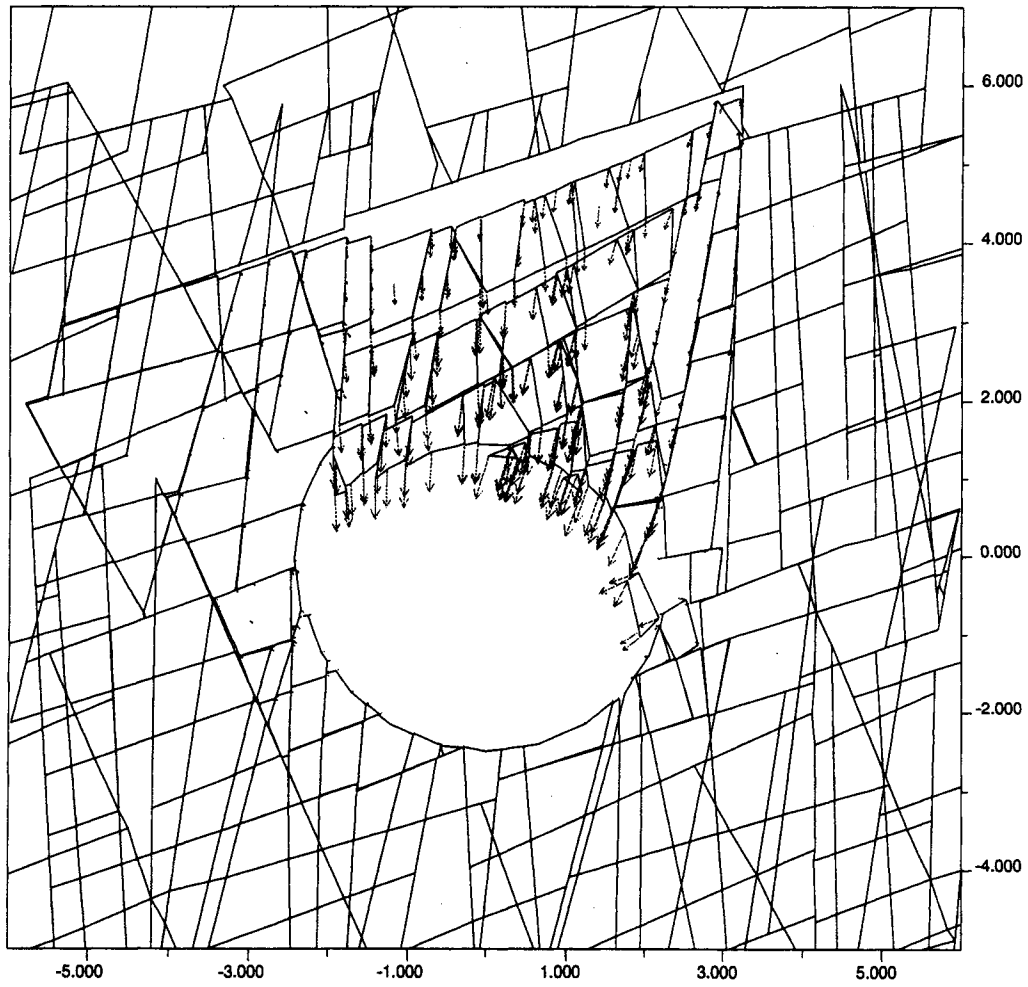

Figure 3-3. Explicit rockfall generated by dynamic simulation after subjecting to one episode of earthquake ground motion for case C (unheated drift)

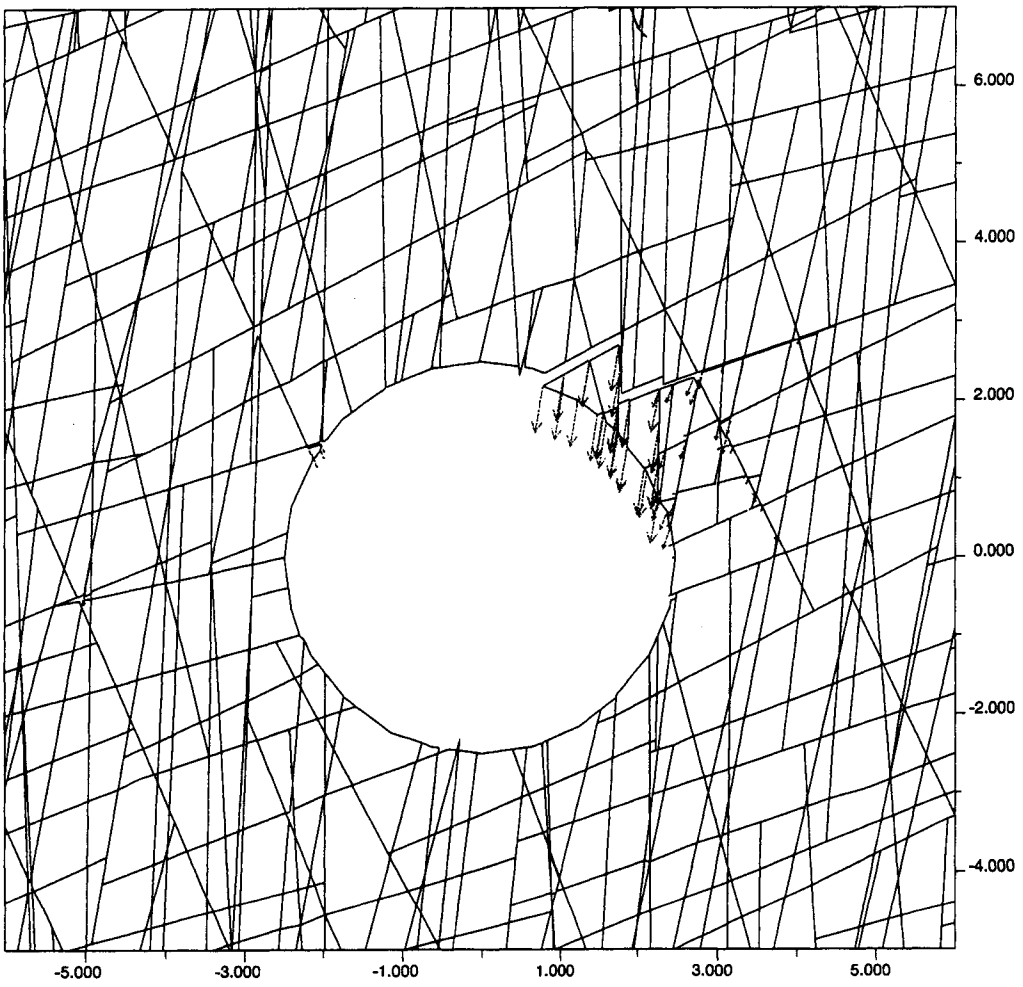

Figure 3-4a. Explicit rockfall generated by thermal and dynamic simulation for case B1 (heated drift) after 100 yr of thermal loading

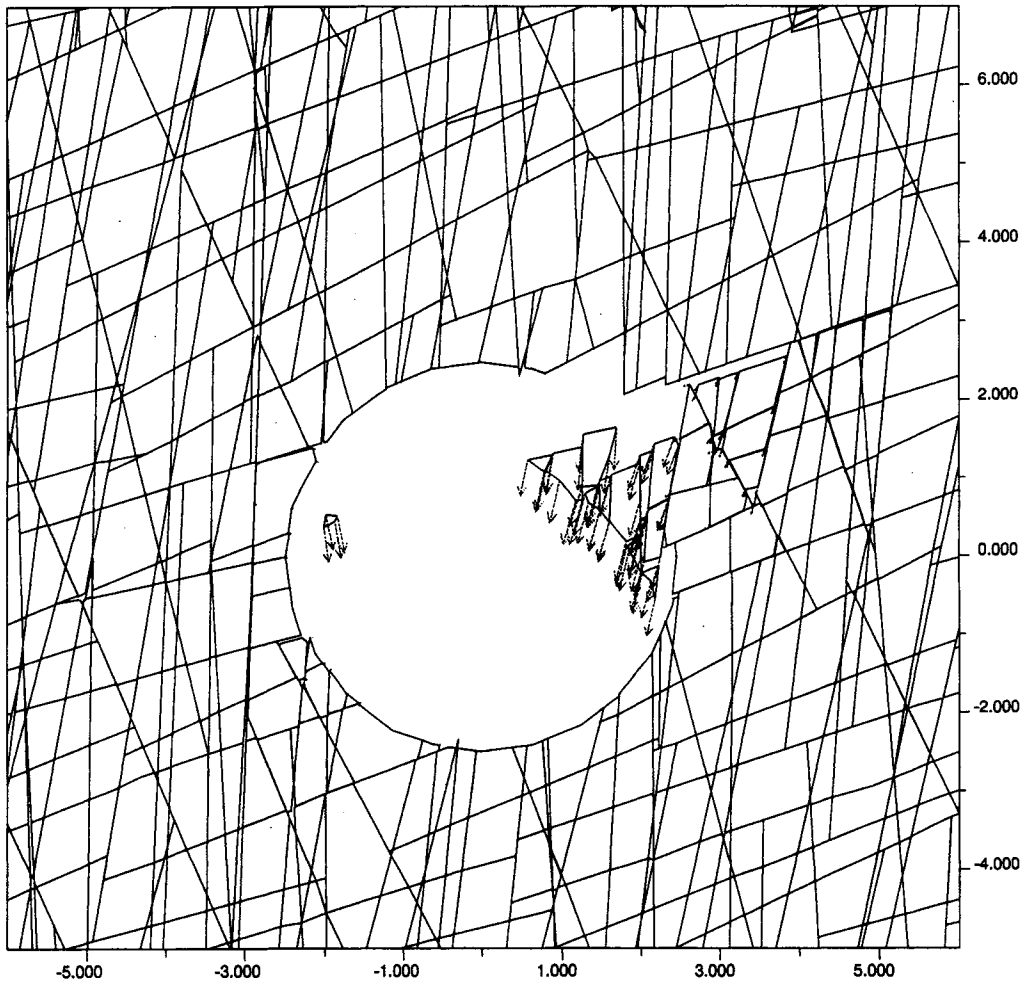

Figure 3-4b. Explicit rockfall generated by thermal and dynamic simulation for case B1 (heated drift) after 100 yr of thermal loading and one episode of earthquake ground motion

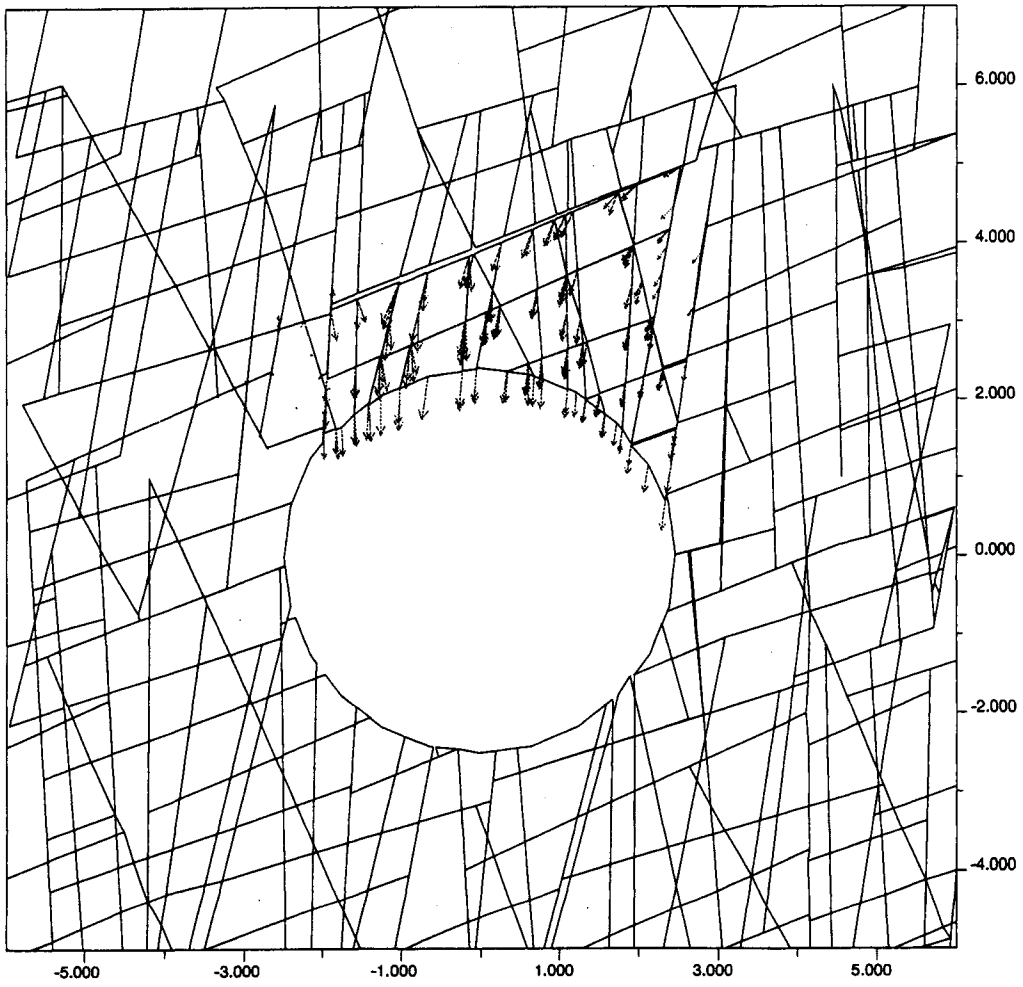

Figure 3-5a. Explicit rockfall generated by thermal and dynamic simulation for case C1 (heated drift) after 100 yr of thermal loading

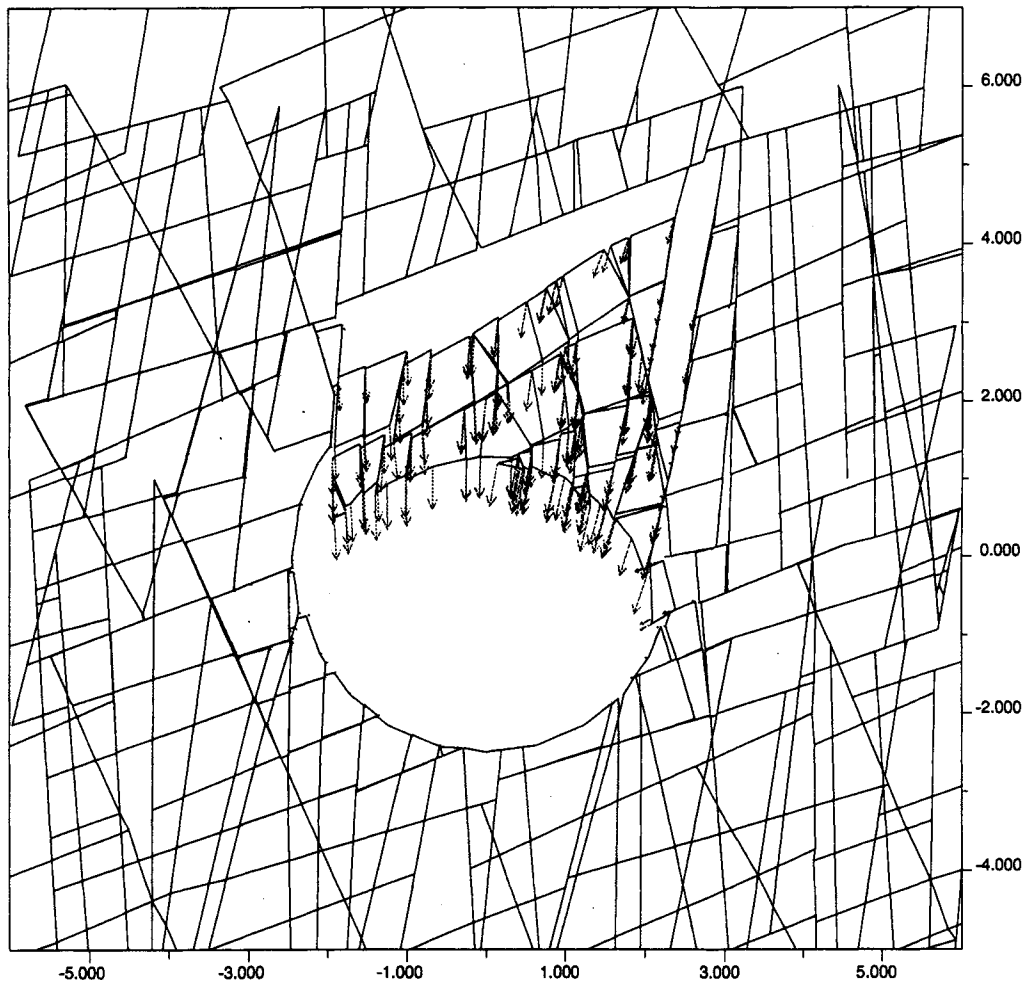

Figure 3-5b. Explicit rockfall generated by thermal and dynamic simulation for case C1 (heated drift) after 100 yr of thermal loading and one episode of earthquake ground motion

3.2 FRACTURE DISPLACEMENT

Thermal loading has been observed to generally increase fracture shear displacement and fracture opening (Ahola et al., 1996). A similar phenomenon was observed in the current modeling analyses. Furthermore, seismic load appears to increase both fracture shear displacement and fracture opening significantly as illustrated by figures 3-6a,b and 3-7a,b. An increase in fracture displacement was observed in all three cases for both heated and unheated drifts. It is not practical, however, to quantify these changes in fracture displacements at the current stage. Further modeling effort is necessary, especially since fracture displacements also depend on *in situ* fracture patterns.

3.3 YIELD OF INTACT ROCK BLOCKS

The yield of intact rock blocks was observed previously to increase with thermal load (Ahola et al., 1996) and if extensive yield had already occurred during thermal loading, seismic load will further increase the yield (Ahola, 1997). Not much yield of intact rock blocks was observed during the current study; this may be because of the relatively lower thermal load. Since the yield of intact rock depends largely on rock TM properties, conclusions with regard to the yield cannot be drawn at this stage. Future studies will consider the effect of fracture and intact rock TM properties.

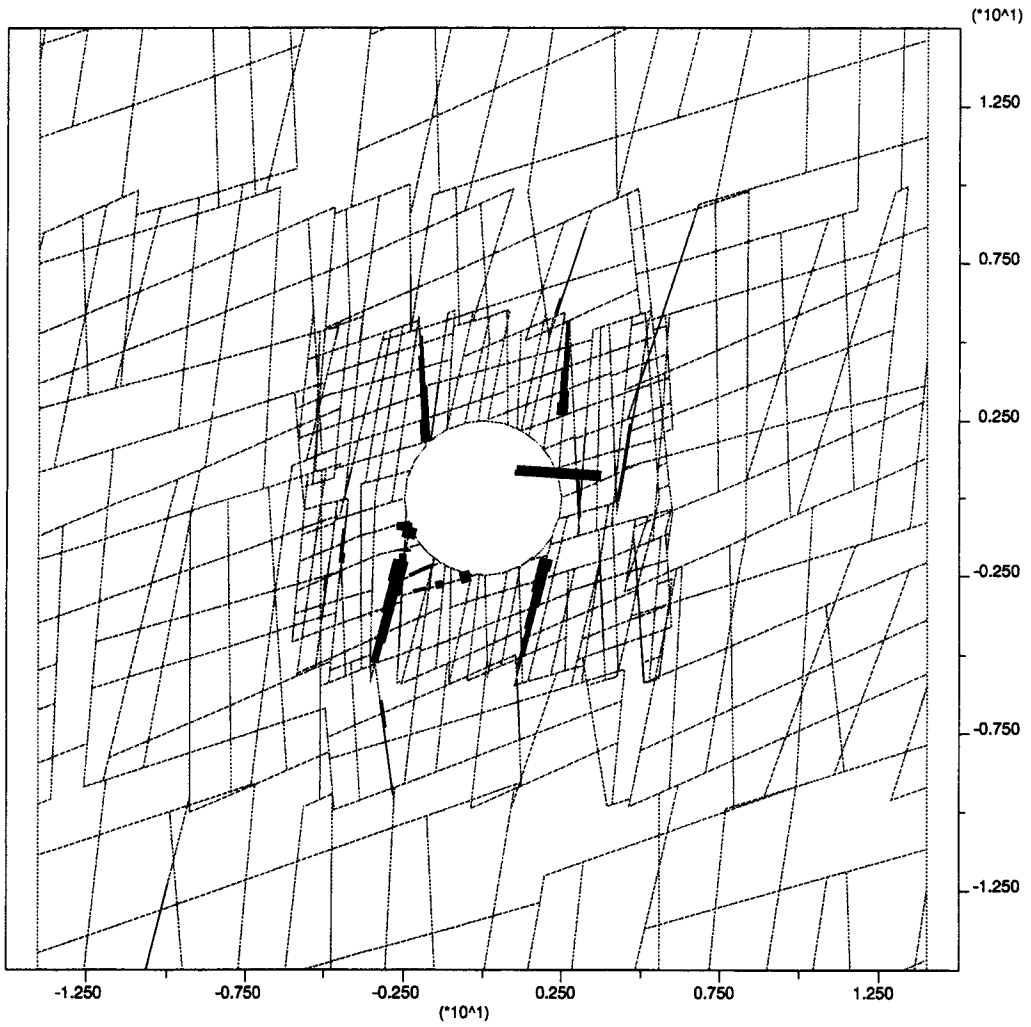

Figure 3-6a. Distribution of fracture shear displacement after drift excavation for case A. Each solid line represents 0.25 mm shear displacement. The number of lines is proportional to the magnitude of shear displacement. Dash lines indicate fracture network.

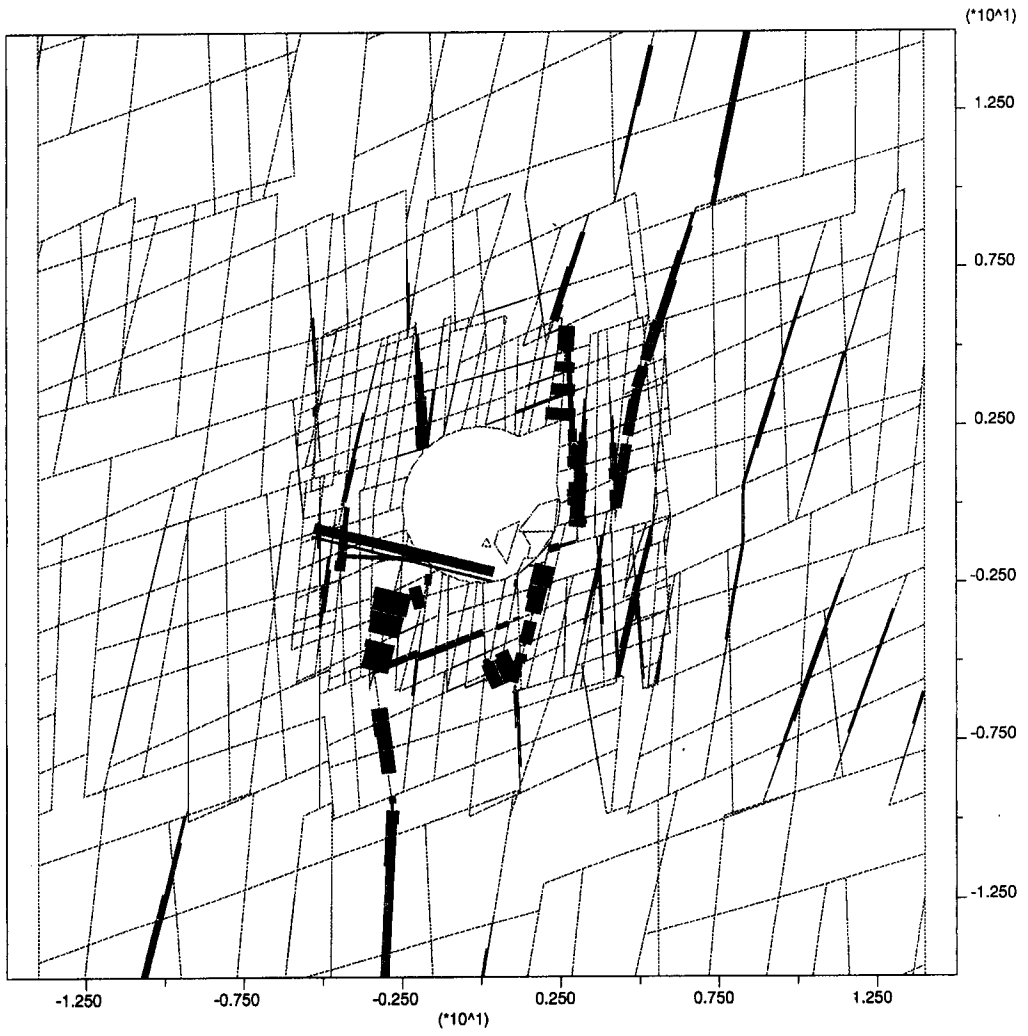

Figure 3-6b. Distribution of fracture shear displacement after one episode of earthquake ground motion for case A. Each solid line represents 0.25 mm shear displacement. The number of lines is proportional to the magnitude of shear displacement. Dash lines indicate fracture network.

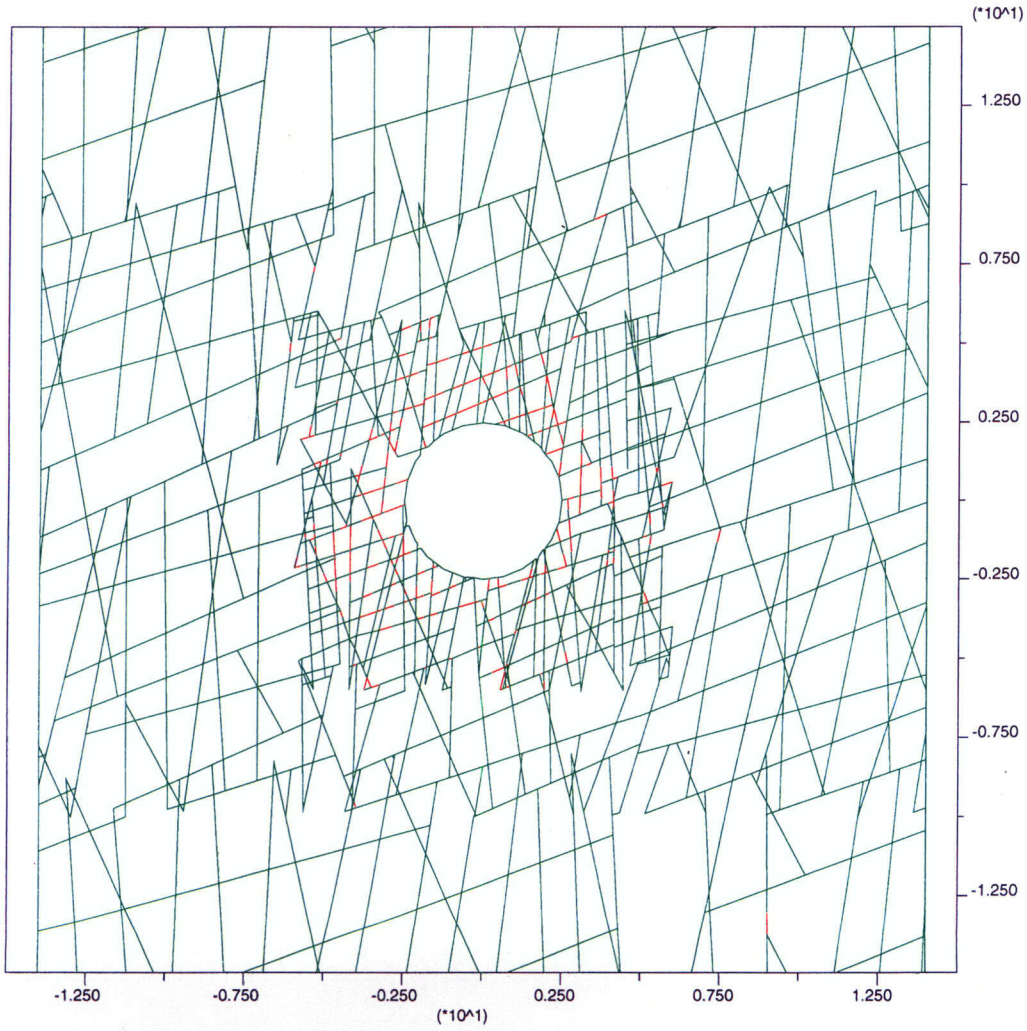

Figure 3-7a. Distribution of opened fractures for case C (in red) after drift excavation

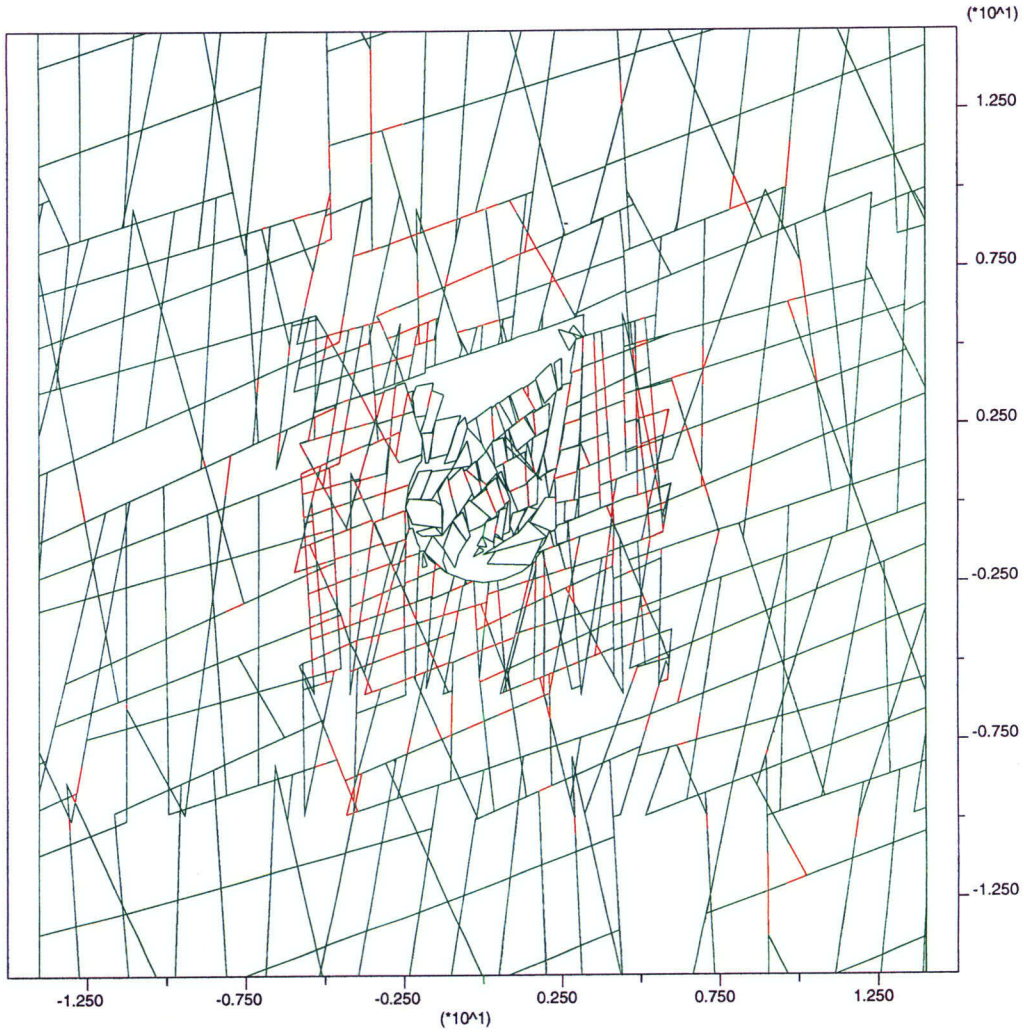

Figure 3-7b. Distribution of opened fractures for case C (in red) after one episode of earthquake ground motion

4 DISCUSSIONS AND FUTURE WORK

4.1 EFFECT OF FRACTURE PATTERN ON ROCKFALL

As discussed earlier, fracture pattern appears to have the controlling effects on the amount of simulated rockfall. With increasing complexity of fracture patterns, especially significantly varying orientations, and decreasing block sizes (or fracture spacings), it appears the number of rock blocks falling on a WP increases. Even with the same set of fracture parameters (i.e., statistical data summarized based on field mapping and other measuring results), the generated fracture pattern could be slightly different. The slight difference in fracture pattern, especially near roof area, could result in a different amount of rockfall during each seismic ground motion episode. The controlling effect of fracture patterns, particularly those of irregular nature, on underground opening stability has been observed in the literature (e.g., Bhasin and Hoeg, 1998; Makurat et al., 1990; Leung and Quek, 1995). It is, therefore, important to be able to characterize fracture distribution and generate fracture patterns representative of the *in situ* fracture pattern at the repository. The fracture generator in Version 3.0 of UDEC is limited to uniform distribution. As mentioned previously, most fracture parameters (e.g., fracture spacing and inclination angle), show a log-normal distribution at YM. Controlling the generated intact block size in the current version of UDEC Version 3.0 is achieved by adjusting the fracture spacing and is not straight forward. Additional external calculations are necessary to estimate the generated block size distribution. Therefore, it is not easy to isolate the effect of block size with similar fracture patterns on rockfall.

Also, fracture patterns may have significant spatial variations within the repository, depending on the nearby stratigraphic and faulting characteristics. It is, therefore, necessary in future studies to consider an array of fracture patterns. To accomplish this, the results of a detailed study of fractures is necessary. Two approaches have been considered: use a more applicable fracture generator and generate fracture patterns based on statistical fracture parameter data from detailed fracture studies and digitize selected fracture mapping results, such as the full-periphery mapping at the ESF main drift with tunnel curvature corrected. The second approach is rather straight forward and relatively easy to interpret. The representiveness of the selected mapped sections may be limited, however. The first approach should be more representative statistically, however, it needs significant effort in identifying and utilizing a practical fracture generator and detailed fracture study using commercial software, such as FRACMAN (Dershowitz et al., 1993). A recently developed technical approach for defining *in situ* block size proposed by Hadjigeorgiou and Grenon (1998) may also be modified and used as a fracture generator.

Another important aspect of the *in situ* fracture geometric characteristic is block size distribution. *In situ* block size distribution is also important in assessing the potential impact of rockfall on WPs—it provides a lower bound for the potential impact force on the WPs by falling blocks. Some research has been done on *in situ* block size at YM. For example, Gauthier et al. (1995) estimated size distribution of individual rock blocks using a modified (log-space) version of the Topopah Spring fracture spacing distribution developed by Schenker et al. (1995), assuming cubic and parallel-piped blocks. It should be noted that assumptions of cubic or parallel-piped block shape may distort the estimation of size distribution of *in situ* blocks through various assumptions with regard to the extent of fractures in the 3D. In published literature in recent years, several models have been developed capable of simulating the 3D nature of a rock mass (e.g., Dershowitz and Einstein, 1988). These models differ in degree of complexity and sophistication and basic theoretical background (e.g., finite/infinite fracture size and block shape). Examples of these models include the Simblock model developed by Peaker (1990), the Blocks model developed by Maerz and Germain (1992),

and the Stereoblock model developed by Hadjigeorgiou et al. (1995) and Hadjigeorgiou and Grenon (1998). These models will be further examined and applied to analyzing block size distributions at YM.

4.2 EFFECT OF SEISMIC TIME HISTORY ON ROCKFALL

As indicated in section 2.1.4, seismic ground motion input in the current modeling study was a sigmoidal dynamic signal to simplify the problem. In an actual earthquake time history, the acceleration pulses are of varying amplitudes and frequencies. Since ground motion at a particular site is influenced by source, travel path characteristics, and local site conditions, it is important in dynamic response analyses to used ground motion input that is site specific. Historically recorded ground motion time histories at YM are currently being selected and analyzed to generate representative site-specific ground motion time histories for continuing dynamic analyses. These three basic steps should be performed in the following order:

(1) Collection and selection of recorded ground motion time histories

(2) Spectrum analyses for source and path characteristics

(3) Generation of a range of site-specific ground motion time histories depicting source and path characteristics

4.3 EFFECT OF INTACT ROCK AND FRACTURE THERMAL-MECHANICAL PROPERTIES

It is recognized that current information and the level of understanding regarding long-term degradation of the rock mass within the near-field repository environment is limited. As a result, the previous parametric study of stability of drift under static load employed ranges of TM parameters measured in the laboratory or field to account for the variation of parameters at the YM site as well as how they may change or degrade with temperature, time, stress, and moisture content (Ahola et al., 1996). The effect of rock and fracture TM properties on stability of drift under dynamic load will be considered and studied in more detail in the future.

4.4 EFFECT OF MODEL SETUP ON ROCKFALL

For block dynamic analysis of a discontinuum system, a few modeling considerations may actually affect modeling results significantly and such effects need to be understood in future modeling exercises. These considerations may include mechanical damping, wave transmission in a discontinuum system, boundary effects, and loading approach. Currently, the performance of the UDEC Version 3.0 code with regard to how these modeling considerations may have affected modeling results is not yet well understood.

4.5 EXPLICIT MODELING OF ROCKFALL AND ROCKFALL CRITERIA

Since the number of computer simulations that can model rockfall explicitly is limited, it is desirable to establish a rock fall criterion to define the vertical extent of the potential rockfall region using indices such as the amount of explicitly simulated rockfall, fracture shear and normal displacements, and yielding of intact rock blocks. Such a rockfall criterion may be a function of fracture pattern, size of *in situ* rock blocks, and level of earthquake ground motion for a specific combination of rock mass TM properties. Future analyses may also explore the dependence of this rockfall criterion on rock mass TM properties.

5 REFERENCES

Ahola, M.P., R. Chen, H. Karimi, S.M. Hsiung, and A.H. Chowdhury. 1996. *A Parametric Study of Drift Stability in Jointed Rock Mass, Phase I: Discrete Element Thermal-Mechanical Analysis of Unbackfilled Drifts.* CNWRA 96-009. San Antonio, TX: Center for Nuclear Waste Regulatory Analyses.

Ahola, M.P. 1997. *A Parametric Study of Drift Stability in Jointed Rock Mass—Phase II: Discrete Element Dynamic Analysis of Unbackfilled Drifts.* CNWRA 97-007. San Antonio, TX: Center for Nuclear Waste Regulatory Analyses.

Anna, L.O. 1998. *Preliminary Three-Dimensional Discrete Fracture Model of Topopah Spring Tuff in the Exploratory Studies Facility, Yucca Mountain Area, Nye County, Nevada.* USGS Open-File Report 97-834. Washington, DC: U.S. Geological Survey.

Beason, S.C. 1997. Previous mapping efforts. *Handout and presentation at U.S. Department of Energy/Nuclear Regulatory Commission Appendix 7 Meetings, October 16, 1997.* Washington, DC.

Bhasin, R., and K. Hoeg, 1998. Parametric study for a large cavern in jointed rock using a distinct element model (UDEC-BB). *International Journal of Rock Mechanics and Mining Sciences* 35(1): 17–29.

Brechtel, C.E., M. Lin, E. Martin, and D. S. Kessel. 1995. *Geotechnical Characterization of the North Ramp of the Exploratory Studies Facility. Vol. 1: Data Summary, Vol. 2: NRC Corehole Data Appendices.* SAND95–0488/1. Albuquerque, NM: Sandia National Laboratories.

Civilian Radioactive Waste Management System, Management and Operating Contractor. 1995. *Controlled Design Assumptions Document.* B00000000–01717–4600-00032. Rev. 02, ICN 01. Las Vegas, NV: Civilian Radioactive Waste Management System.

Civilian Radioactive Waste management System, Management and Operating Contractor. 1996a. *Thermal Loading Study for FY1996.* B00000000–01717–5705–00044. Rev. 1. Las Vegas, NV: Civilian Radioactive Waste Management System.

Civilian Radioactive Waste Management System, Management and Operating Contractor. 1996b. *Mined Geologic Disposal System Advanced Conceptual Design Report.* Volume II. B00000000–0717–5705–00015. Rev. 00. Las Vegas, NV: Civilian Radioactive Waste Management System.

Dershowitz, W.S., and H.H. Einstein. 1988. Characterizing rock joint geometry with joint system models. *Rock Mechanics* 21: 21–51.

Dershowitz, W., G. Lee, J. Geier, S. Hitchcock, and P. LaPointe. 1993. *FRACMAN-Interactive Discrete Feature Data Analysis, Geometric Modeling, Exploration Simulation.* Redmond, WA: Golder Associates Inc.

Gauthier, J.H., M.L. Wilson, D.J. Borns, and B.W. Arnold. 1995. Impacts of seismic activity on long-term repository performance at Yucca Mountain. *Focus '95: Proceedings of the Methods of Seismic Hazards Evaluation.* La Grange Park, IL: American Nuclear Society: 159–168.

Hadjigeorgiou, J., and M. Grenon. 1998. Defining in-situ block size. *The Canadian Mining and Metallurgical Bulletin* 91(1020): 72–75.

Hadjigeorgiou, J., J.F. Lessard, and F. Flament. 1995. Characterizing in-situ block distribution using a stereological model. *Canadian Tunneling Journal*: 201–211

Itasca Consulting Group, Inc. 1996. *UDEC—Universal Distinct Element Code. Version 3.0, Volume I: User's Manual.* Minneapolis, MN: Itasca Consulting Group, Inc.

Leung, C.F., and S.T. Quek. 1995. Probabilistic stability analysis of excavations in jointed rock. *Canadian Geotechnical Journal* 32: 397–407.

Lin, M., M.P. Hardy, and S.J. Bauer. 1993. *Fracture Analysis and Rock Quality Designation Estimation for the Yucca Mountain Site Characterization Project.* SAND92–0449. Albuquerque, NM: Sandia National Laboratories.

Maerz, N.H., and P. Germain. 1992. Block size determination around underground openings using simulations based on scanline mapping. *Preprints of the International Society for Rock Mechanics Conference on Fractured and Jointed Rock Masses, Lake Tahoe, Nevada.* Berkeley, CA: Lawrence Berkeley National Laboratory.

Makurat, A., N. Barton, G. Vik, P. Chryssanthakis, and K. Monsen. 1990. *Rock Joints.* Barton and Stephansson, eds. ISBN 90 61901 1095. Balkema, Rotterdam.

Peaker, S.M. 1990. *Development of a simple block size distribution model for the classification of rock masses.* Master's thesis, University of Toronto.

Pye, J.H., D.C. Kicker, and G.H. Nieder-Westermann. 1997. Plans for mapping of subsurface Facilities. *Notes from U.S. Department of Energy/Nuclear Regulatory Commission Appendix 7 Discussions. October 16, 1997.* Washington, DC.

Schenker, A.R., D.C. Guerin, T.H. Robey, C.A. Rautman, and R.W. Barnard. 1995. *Stochastic Hydrogeologic Units and Hydrogeologic Properties Development for Total-System Performance Assessments.* SAND94–0244. Albuquerque, NM: Sandia National Laboratories.

Scott, R.B., and M. Castellanos. 1984. *Stratigraphic and Structural Relations of Volcanic Rocks in Drill Holes USW GU–3 and USW G–3, Yucca Mountain, Nye County, Nevada.* USGS/OFR–84–491 (NNA.890804.0017, USW GU–3) Denver, CO: U.S. Geological Survey.

Spengler, R.W., D.C. Muller, and R.B. Livermore. 1979. *Preliminary Report on the Geology and Geophysics of Drill Hole UE–25a–1, Yucca Mountain Nevada Test Site.* USGS/OFR–79–1244 (HQS.880517.1491) (UE–25a #1). Denver, CO: U.S. Geological Survey.

Spengler, R.W., and J.G. Rsenbaum. 1980. *Preliminary Interpretations of Geologic Results Obtained from Boreholes UE25a–4, –5, –6, and –7, Yucca Mountain, Nevada Test Site.* USGS/OFR–80–929 (NNA.890823.0106). Reston, VA: U.S. Geological Survey.

Spengler, R.W., F.M. Byers, Jr., and J.B. Warner. 1981. *Stratigraphy and Structure of Volcanic Rocks in Drill Hole USW–G1, Yucca Mountain, Nye County, Nevada.* USGS/OFR–81–1349, DOE/ET/44802/T4 (HQS.880517.1492) (USW G–1). Denver, CO: U.S. Geological Survey.

Spengler, R.W., M.P. Chornack, D.C. Muller, and J.E. Kibler. 1984. *Stratigraphic and Structural Characteristics of Volcanic Rocks in Core Hole USW G–4, Yucca Mountain, Nye County, Nevada.* USGS/OFR–84–789 (NNA.870519.0105) (USW G–4). Denver, CO: U.S. Geological Survey.

Sweetkind, D.S., and S.C. Williams-Stroud. 1996. *Characteristics of Fractures at Yucca Mountain, Nevada: Synthesis Report.* Administrative Report. Denver CO: U.S. Geological Survey.

TRW Environmental Safety Systems, Inc. 1994a. *Initial Summary Report for Repository/Waste Package Advanced Conceptual Design.* B00000000–01717–5705–00015. Volume I, Rev. 00. Las Vegas, NV: TRW Environmental Safety Systems, Inc.

TRW Environmental Safety Systems, Inc. 1994b. *FY93 Thermal Loading Systems Study Final Report.* Volumes II and II, Rev. 1. Las Vegas, NV: TRW Environmental Safety Systems, Inc.

TRW Environmental Safety Systems, Inc. 1995. *Thermomechanical Analyses.* Prepared for the U.S. Department of Energy. BC0000000–0717–5705–00013. Rev. 00. Las Vegas, NV: TRW Environmental Safety Systems, Inc.

TRW Environmental Safety Systems, Inc. 1996. *Thermal Loading Study for FY1995.* Las Vegas, NV: TRW Environmental Safety Systems, Inc.

U.S. Department of Energy. 1994. *Reference Information Base (RIB), Yucca Mountain Site Characterization Project.* Washington, DC: U.S. Department of Energy.

U.S. Department of Energy. 1998. *Repository Thermal Loading Management Analysis.* B00000000–01717–0200–00135. Rev. 00. Washington, DC: U.S. Department of Energy.

Wernicke, B.P. 1992. Cenozoic extensional tectonics of the Western Cordillera. The Cordilleran Orogen: Conterminous U.S. B.C. Burchfiel, P.W. Lipman, and M.C. Zoback, eds. *The Geology of North America.* Boulder, CO: Geological Society of America G-3: 553–581.

Wong, I.G., and J.C. Stepp. 1998. *Probabilistic Seismic Hazard Analyses for Fault Displacement and Vibratory Ground Motion at Yucca Mountain, Nevada.* Final report. Oakland, CA: Civilian Radioactive Waste Management System.